

Perfluorooctane Sulphonate-Induced Hepatic Ultrastructural Changes in Rats Ameliorated by Quercetin Via its Antioxidant-Defense Action

Original
Article

Dalia A. Mandour, Marwa Sabry Abd El-Aal, Ibrahim Amin Ibrahim and Rania Said Moawad

Department of Human Anatomy & Embryology, Faculty of Medicine, Zagazig University, Egypt

ABSTRACT

Introduction: Perfluoroalkyl and polyfluoroalkyl substances (PFASs) are manufactured fluorinated chemicals, including Perfluorooctane sulfonate (PFOS) and Perfluorooctanoic acid (PFOA), they cause dormant environmental toxicity. Quercetin (QE), one of the major flavonoids, present in numerous food, has anti-oxidants and anti-inflammatory properties.

Aim of the Study: The study aimed to clarify the potential hepatoprotective role of QE against PFOS-induced liver histological and immunohistochemical changes in adult male albino rats.

Materials and Methods: Thirty-six adult male albino rats were randomly and equally distributed into three groups: Control group, PFOS-treated group: were received PFOS (20 mg/kg/day) by oral gavage for 28 days and PFOS+QE group: were received PFOS (20 mg/kg/day) and QE (75 mg/kg/day) by oral gavage for 28 days. At the end of the experiment, the rats in all groups were anesthetized, sacrificed, and the livers were processed for biochemical, histological, and immunohistochemical study.

Results: In the PFOS-treated group, body weight, superoxide dismutase (SOD), glutathione peroxidase (GPX), and catalyze (CAT) levels significantly decreased while liver weight, liver function tests (LFTs), malondialdehyde (MDA), and C-reactive protein (CRP) levels were significantly increased. Microscopically, liver sections of the PFOS-treated group exhibited inflammatory cellular infiltration, hepatocytes with vacuolation, abnormally shaped nuclei and swollen mitochondria. Also, strong positive reactions for Caspase 3 and tumor necrosis factor-alpha (TNF- α) were detected. The PFOS+QE group displayed a significant resetting of the biochemical parameters and a partial extenuation of the light, electron, and immunohistochemical changes.

Conclusion: This work could highlight the possibility of using QE as a preventative strategy for potential PFOS-induced hepatic toxicity.

Received: 17 May 2022, **Accepted:** 05 July 2022

Key Words: Cytoarchitecture, histopathology Quercetin, liver, perfluorooctane sulfonate, rat.

Corresponding Author: Rania Said Moawad, MD, Department of Human Anatomy & Embryology, Faculty of Medicine, Zagazig University, Egypt, **Tel.:** +20 10 6000 3278, **E-mail:** karimwaleed62@gmail.com

ISSN: 1110-0559, Vol. 46, No. 3

INTRODUCTION

Perfluoroalkyl substances (PFASs) are synthetic compounds belonging to the persistent organic pollutants class (POPs)^[1,2]. Perfluoroalkyl substances exhibit a variety of anti-wetting and surfactant-like characteristics. They are used in non-stick cookware, breathable textiles, waterproofing, and firefighting foams, as well as protective coatings for paper and food packaging material manufacture^[3]. Additionally, they are utilized in stain- and water-resistant fabrics, carpeting, paints, and cleaning treatments. Furthermore, PFASs are used in various industries, such as aerospace, automotive, construction projects, and electronics^[4]. Food and Drug Administration (FDA) has authorized a restriction on the use of PFASs in food packaging, cookware, and food processing equipment^[5].

Among PFASs, Perfluorooctane sulfonate (PFOS) has most frequently been detected as dominant PFASs in

environmental and biological samples^[6,7]. It is widely used in consumer products like furniture, household cleaners, and clothing. Due to its resistance to environmental and metabolic degradation, it was also categorized as (POPs) in 2009 under the Stockholm Convention^[8,9,10]. Human exposure occurs through different sources, including the food chain, dust ingestion, air inhalation, and drinking water^[11-15].

Quercetin (QE) is a flavonoid compound found in numerous foods, such as onions, apples, strawberries, tea, and coffee^[16-19]. Quercetin was reported to be beneficial for those suffering from health issues such as renal^[20], neurogenic^[21], and cardiac disorders^[22]. Quercetin possesses several features, such as anti-oxidant activity and anti-inflammatory activity^[23-26]. Many studies have established the favorable role of flavonoids, particularly QE, in improving hepatic insults^[27-29]. Quercetin is now used as a nutritive supplementation and as a phytochemical

therapy for many hepatic dysfunctions, such as acute liver failure, hepatitis, alcoholic liver disease, fatty liver, cirrhosis, steatosis, cancer, and portal hypertension^[30].

Consequently, this study was done to elucidate QE's hepatoprotective activity against the biochemical, histological, and immunohistochemical changes induced by oral PFOS in adult male albino rat.

MATERIALS AND METHODS

Chemicals

PFOS: White, odourless powder purchased from Sigma-Egypt (Nasr city, Cairo) and was dissolved (5 mg / ml of distilled water).

Quercetin (QE): was obtained from Sigma-Egypt (Nasr city, Cairo) in the form of a yellow powder and was dissolved (15 mg / ml of distilled water).

Animals

Mature male albino rats weighing approximately 180 to 250 grams, aging 3-5 months were used in this study. The rats were kept in a well-ventilated area with a 12-hour light/dark cycle and unrestricted access to food and drinking water. All laboratory techniques were approved by the Institutional Animal Care and Use Committee of Zagazig University, Egypt (IACUC, approval number: Zu-IACUC/3/F/27/2019).

Experimental design

Thirty-six rats were distributed equally into three groups:

Group I (control group): Negative control rats (n= 6): were supplemented with regular diet and distilled water for 28 days.

Positive control rats (n=6): were supplemented orally with gavage of QE (75 mg/kg BW) for 28 days^[31].

Group II (PFOS-treated group): Rats were received oral gavage with PFOS (20 mg/kg BW) for 28 days^[32].

Group III (PFOS+QE group): Rats were received oral gavage with PFOS (20 mg/kg BW) and QE (75 mg/kg BW) for 28 days.

After 28 days, the weight of rats in each group was estimated then, they were anesthetized by intraperitoneal injection of 100 mg/kg of thiopental^[33]. Venous blood samples were taken from retro-orbital venous plexus, left to clot, then centrifuged at 3000 r.p.m to collect the serum. Then serum levels of liver function tests, including Alanine aminotransferase (ALT), aspartate aminotransferase (AST), Alkaline phosphatase (ALP), were measured in the central lab, Faculty of Veterinary, Zagazig University. Thereafter, abdominal incision was done, and the left lobe was dissected out from each rats' abdomen. The livers were weighed and dissected into specimens. Some specimens were processed for tissue homogenates to assess Superoxide Dismutase (SOD), Glutathione Peroxidase

(GPX), Malondialdehyde (MDA), and C reactive protein (CRP). At the same time, other specimens were processed for light, electron microscopic, and immunohistochemical analysis.

Biochemical Study

Assessment of liver function tests (LFTs)

Serum ALT in (U/L) and AST in (U/L) were detected by the method of Reitman and Frankel (1957)^[34], and ALP in (U/L) was determined by Lowry *et al.* (1951)^[35] method.

Assessment of liver tissue homogenate

Utilizing a glass homogenizer, liver specimens from all groups were homogenized in a lysis buffer containing 10mM Tris-HCl, 150mM NaCl, 10mM sucrose, and 0.1mM EDTA pH 7.4. Centrifugation at 3000 rpm for 10 minutes at 4°C was performed. The supernatants were collected, and the protein concentration of the tissue homogenates was determined using the Bradford method^[36]. The hepatic levels of SOD^[37], GPX^[38], CAT^[39], MDA^[40], and CRP were determined using ELISA kits following the manufacturer's instructions (Westing Biotechnology, Shanghai, China)^[31].

Light microscopic study

Left lobe specimens were fixed in 10% buffered formalin and processed for paraffin wax insertion and sectioning into sequential 5µm thick sections by the method of Bancroft and Layton (2018)^[41]. The liver sections were stained with hematoxylin and eosin (H&E) and afterward examined utilizing a light microscope (the Leica DM500) equipped with a digital camera (the Leica ICC50 W Camera Modul).

Immunohistochemical study

The sections were deparaffinized, rehydrated, and immersed in 3% hydrogen peroxide for ten minutes. To facilitate antigen retrieval, sections were soaked in an antigen retrieval solution (10 mmol/l sodium citrate buffer, pH 6) for 20 minutes before being microwaved for another 20 minutes. Treatment with phosphate buffer solution (PBS) and 10% normal goat serum decreased non-specific protein binding. Phosphate buffer solution was used to incubate the slides for 2 hours with the primary anti-rabbit-antibody for Caspase-3 (diluted at 1/500) and primary anti-rat antibody for TNF-α (diluted at 1/200). Subsequently, a biotinylated monoclonal secondary antibody was introduced (diluted 1/100). After adding drops of streptavidin peroxidase for 20 minutes, the slides were rinsed with PBS for 5 minutes. The slides were chromogenically treated with diaminobenzidine and afterward washed with distilled water. Eventually, slides were counterstained with hematoxylin and examined using a light microscope equipped with a Leica DM 500, Microsystems, AG, Heerbrugg, CH-9435, Switzerland, in the Anatomy Department, faculty of medicine, Zagazig University, Egypt. The brown color showed a positive reaction in cytoplasm of hepatocytes. Phosphate buffer solution was used as a negative control in place of the

primary antibody. Positive controls from the appendix for TNF- α and from tonsils for Caspase 3 were used^[42].

Transmission electron microscopic study

Very small liver specimens were immediately fixed for two hours at 4°C with 2.5 % glutaraldehyde in 0.1mol/l cacodylate buffer at pH 7.4. After rinsing with buffer, the specimens were post-fixed for Two hours at 4°C in 1% osmium tetroxide in distilled water. Employing the Glauert and Lewis (2014)^[43] technique, the specimens were processed and placed in EMBED-812 resin in BEEM capsules for 24 hours at 60°C. Afterward, ultrathin sections of 70–90 nm in thickness were cut and stained with uranyl acetate and lead citrate. The specimens were investigated using a JEOL 1010 microscope (Com., Tachikawa, Tokyo, Japan) equipped with a digital integrated Gatan camera at Al-Mansoura University's electron microscope unit.

Morphometric analysis

Immunostained sections for positive Caspase-3 and TNF- α were morphometrically analysed in the histology department, Zagazig University, Egypt. The mean area percentage of Caspase-3 and TNF- α immune reaction was measured in ten fields from each rat at total magnification X400 using Fiji image J image analysis software (National Institute of Health; NIH, Bethesda, MD, USA).

Statistical study

Statistical analyses were conducted employing the SPSS program version 16.0 (Statistical Package for Social Science). Because the data had a normal distribution, continuous variables were represented by the mean and standard deviation (parametric). ANOVA was conducted to determine the significance of differences between groups, followed by LSD (Least significant difference) as a post hoc test to assess the importance of variables between two investigated groups. A *P* value of 0.05 implied that the findings are significant, while the 0.01 implies that the results are highly significant^[44].

RESULTS

Body Weight, Liver weight, and relative liver weight assessment

It was found that there was a highly statistically significant decrease in the body weight in Group II (PFOS-treated) (174 ± 10.46) in comparison to that of control (212 ± 11.35) and PFOS+QE groups (195 ± 10.51). No significant statistical difference was detected between PFOS+QE, and control groups, (Figure 1a).

Liver and relative liver weight (weight of liver divided by the whole-body weight); showed a highly statistically significant increase in Group II (PFOS-treated) (17.15 ± 0.68 , 9.8 ± 1.24) compared to control (8.01 ± 0.46 , 3.7 ± 0.41) and PFOS+QE groups (8.38 ± 1.01 , 4.2 ± 0.53) respectively. Also, no significant statistical difference was detected between PFOS+QE, and control groups, (Figures 1 b, c).

ALT, AST, and ALP levels assessment

Concerning ALT, AST, and ALP levels in Group II (PFOS-treated), they were (134.42 ± 9.27 , 128.90 ± 9.27 , 146.83 ± 14.52) and showed a highly significant increase compared to control (59.22 ± 2.78 , 85.23 ± 5.51 , 52.14 ± 3.61) and PFOS+QE groups (62.56 ± 3.13 , 90.05 ± 5.27 , 58.69 ± 9.1) respectively. In addition, no significant statistical difference was detected between PFOS+QE, and control groups, (Figure 2).

SOD, GPX and CAT (Anti-oxidant enzymes), MDA, and CRP levels evaluation

Concerning SOD, GPX, and CAT levels, Group II (PFOS-treated) showed a highly significant decrease (9.63 ± 1.51 , 13.5 ± 1.15 , 22.75 ± 2.65). In contrast, MDA (107.5 ± 13.35) and CRP (2.80 ± 0.35) levels showed a highly significant increase compared to control (30.2 ± 2.49 , 28 ± 2.16 , 53.2 ± 3.12 , 53.5 ± 5.5 , 0.8 ± 0.11) and PFOS+QE groups (29.45 ± 1.25 , 26.95 ± 0.83 , 52.1 ± 4.18 , 60.1 ± 4.19 , 0.93 ± 0.06) respectively. Also, a nonsignificant difference was detected between control and PFOS+QE groups regarding SOD, GPX, and CAT, MDA and CRP levels, (Figures 3 a,b,c,d).

Light microscopic results

Examination of H&E liver-stained sections of Group I (-ve and +ve control group) revealed the same histological picture. The hepatic lobules showed hepatic cords arising from the central vein. Narrow radiating blood sinusoids were presented among hepatic cords. Cords were formed of polygonal hepatocytes with acidophilic cytoplasm and vesicular nuclei (Figure 4A). The portal area with portal venule and bile ductule, was located at the periphery (Figure 4B).

H&E liver-stained sections of Group II (PFOS-treated group) showed apparently dilated congested central vein with a partial detachment of its endothelium (Figure 5A). Some hepatic lobules showed focus of mononuclear cellular infiltration close to the congested central vein (Figure 5B). Some hepatocytes were with ballooning, and vacuolated cytoplasm, others were with darkly stained shrunken nuclei. There was an area of hepatocytes lost their nuclei. Some blood sinusoids were dilated and congested (Figure 5C). Portal venule was dilated and congested; mononuclear cellular infiltration, multiple dilated bile ductules, and stratification of bile ductular epithelium were also seen (Figure 5D).

H&E liver-stained sections of group III (PFOS+QE group) revealed; most hepatocytes had acidophilic cytoplasm and vesicular nuclei. Hepatocytes were arranged in cords arising from the central vein. Some sinusoids among hepatic cords were dilated, but other sinusoids were apparently normal (Figure 6A). Normal portal venule and bile ductules, and some inflammatory cells still seen (Figure 6B).

Immunohistochemical results

Immunohistochemically stained sections of the control groups presented negative immune reactions for Caspase-3 in the hepatocyte's cytoplasm (Figure 7A). Also, they were negative for TNF- α in the hepatocyte's cytoplasm and in the sinusoid wall (Figure 8A). However, the PFOS-treated group presented strong positive reactions for Caspase-3 in the hepatocyte's cytoplasm (Figure 7B) and for TNF- α in the hepatocyte's cytoplasm and in the sinusoids wall (Figure 8B). Group III (PFOS+QE group) presented moderate positive immunoreactions for Caspase-3 in the hepatocyte's cytoplasm (Figure 7C) and for TNF- α in the sinusoid wall (Figure 8C).

Morphometric results

In comparison to the control groups, the PFOS-treated and PFOS+QE groups demonstrated a markedly significant increase in the mean area percentage of Caspase-3 and TNF- α immunoreactions ($P < 0.001$). The PFOS+QE group demonstrated a substantially significant decrease in comparison to the PFOS-treated group ($P < 0.001$), as shown in (Figure 9).

Transmission Electron microscopic results

Electron microscopic study of group I (control groups) showed normal hepatocytes with euchromatic nuclei, and intact nuclear membrane. Their cytoplasm contained mitochondria, ribosomes, and lysosomes (Figure 10A).

Bile canaliculi containing microvilli occupying their lumina and normal tight cell to cell junction were observed (Figure 10B).

Electron microscopic examination of the liver section of group II (PFOS-treated group) showed hepatocytes with heterochromatic nuclei with irregular nuclear membrane, and the cytoplasm contained multiple swollen mitochondria and some vacuolations (Figure 11A). Binucleated hepatocytes with extensive vacuolations were seen. Its cytoplasm also had multiple disrupted mitochondria and some lipid droplets. The cell boundary of the hepatocyte showed areas of collagen deposits. Depletion of glycogen granules was also seen (Figure 11B). The cytoplasm contained swollen and abnormally shaped mitochondria and some lysosomes. Bile canaliculus was with dilated lumen. Tight Cell to cell junction was still seen (Figure 11C).

Electron microscopic study of liver sections of group III (PFOS+QE group) showed improvement of hepatic ultrastructure when compared to the treated group. Most hepatocytes appeared with euchromatic nuclei and intact nuclear membrane. The cytoplasm contained numerous mitochondria and some lysosomes. Rarefied area of the cytoplasm was still present. Some vacuolations (V) were still seen in the cytoplasm (Figure 12A). Some bile canaliculi had microvilli that occupied their lumen, while others had degenerated microvilli with a wide lumen. Tight cell to cell junction was also seen (Figure 12B).

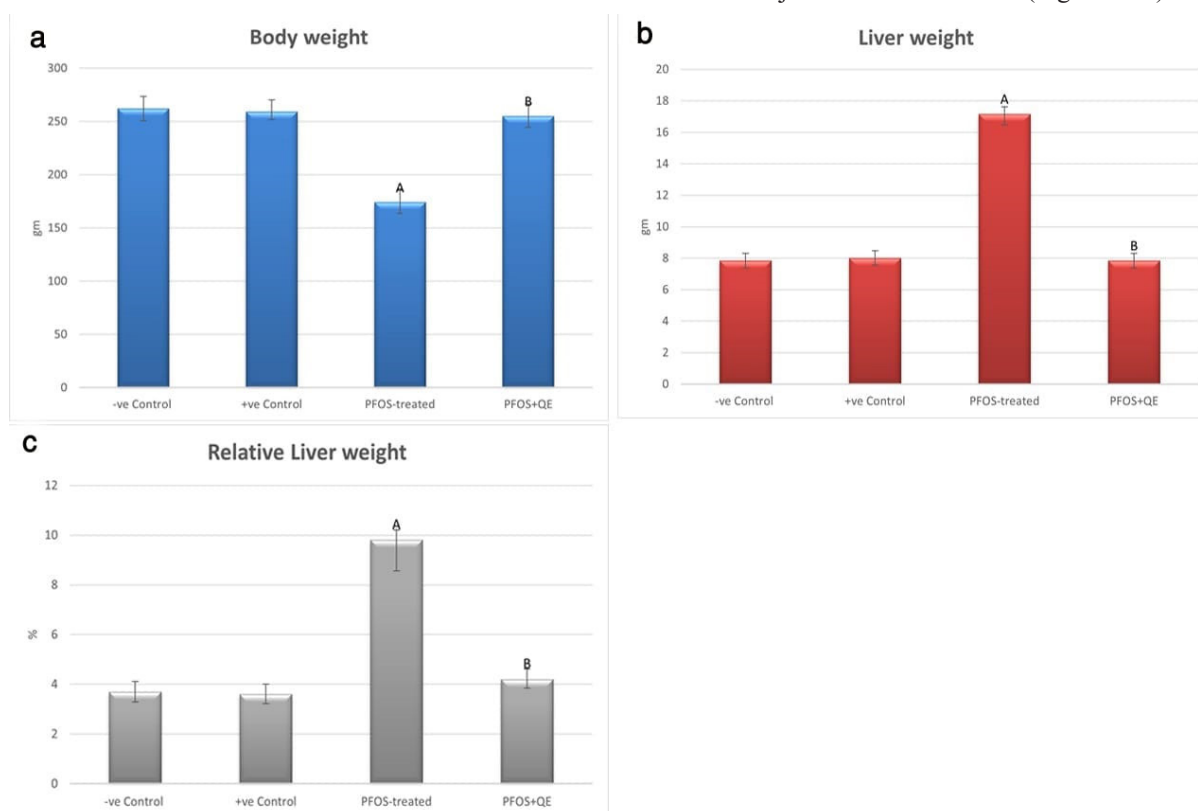


Fig. 1: Histograms showing the comparison between different studied groups regarding (a) body weight (gm), (b) liver weight (gm), (c) relative liver weight (%) respectively.

A highly significant difference with control groups ($P < 0.001$).

B highly significant difference with the PFOS-treated group ($P < 0.001$).

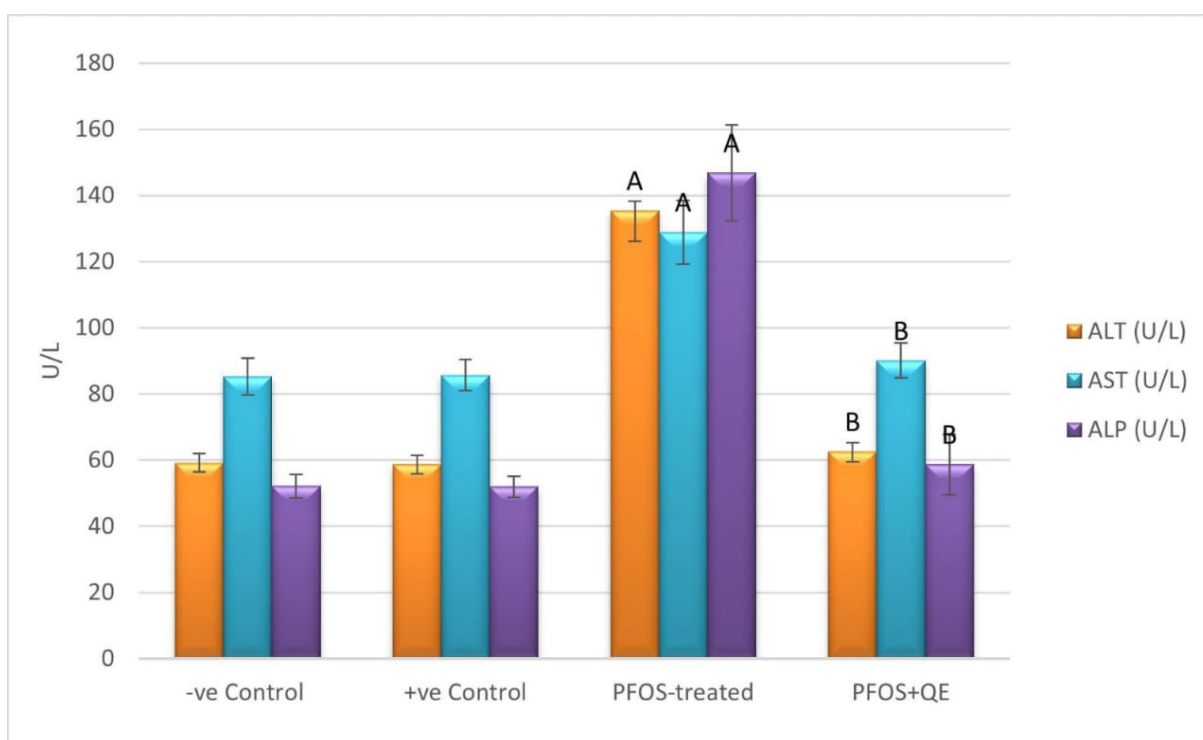


Fig. 2: Histogram showing the comparison between different studied groups regarding LFTs (ALT, AST&ALP) (U/L).
 A highly significant difference with control groups ($P<0.001$).
 B highly significant difference with the PFOS-treated group ($P<0.001$).

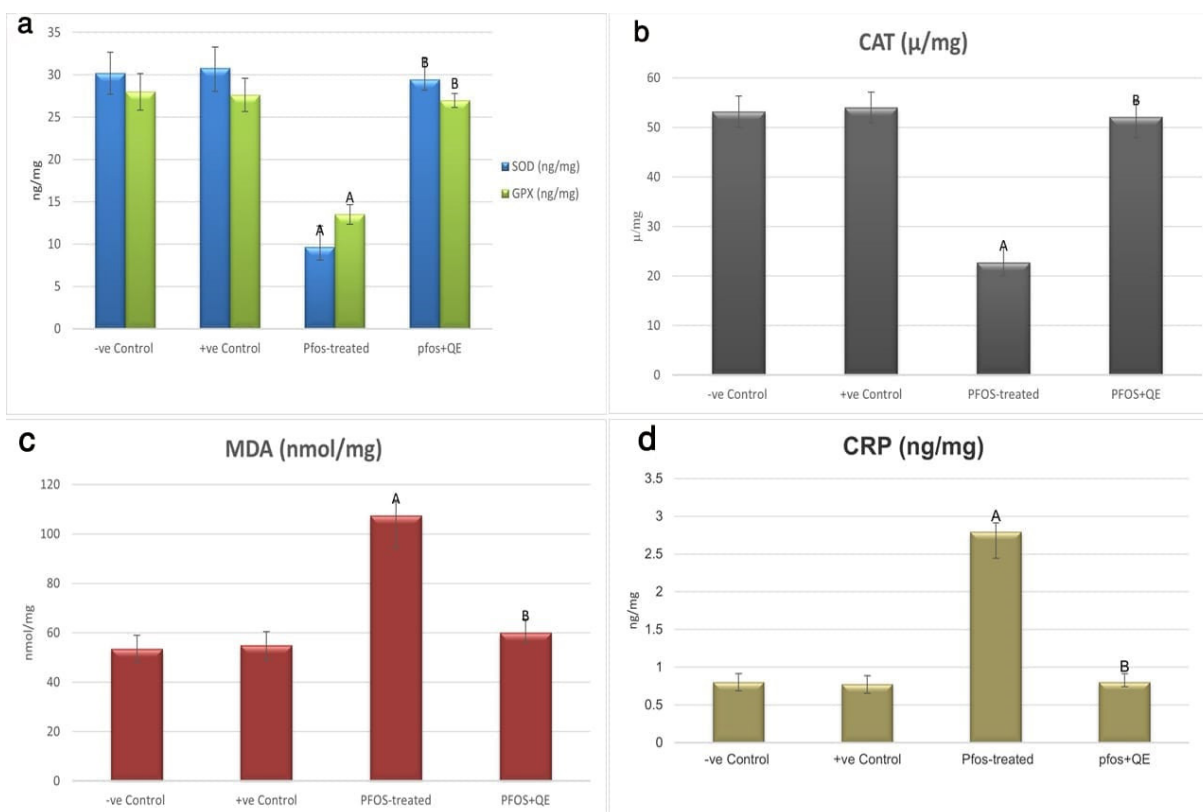


Fig. 3: (a): Histogram showing the comparison between different studied groups regarding antioxidant enzymes (SOD, GPX) (ng/mg). (b): Histogram showing the comparison between different studied groups regarding CAT activity (μ /mg). (c): Histogram showing the comparison between different studied groups regarding (MDA) (nmol/mg). (d): Histogram showing the comparison between different studied groups regarding (CRP) (ng/mg).
 A highly significant difference with control groups ($P<0.001$).
 B highly significant difference with the PFOS-treated group ($P<0.001$).

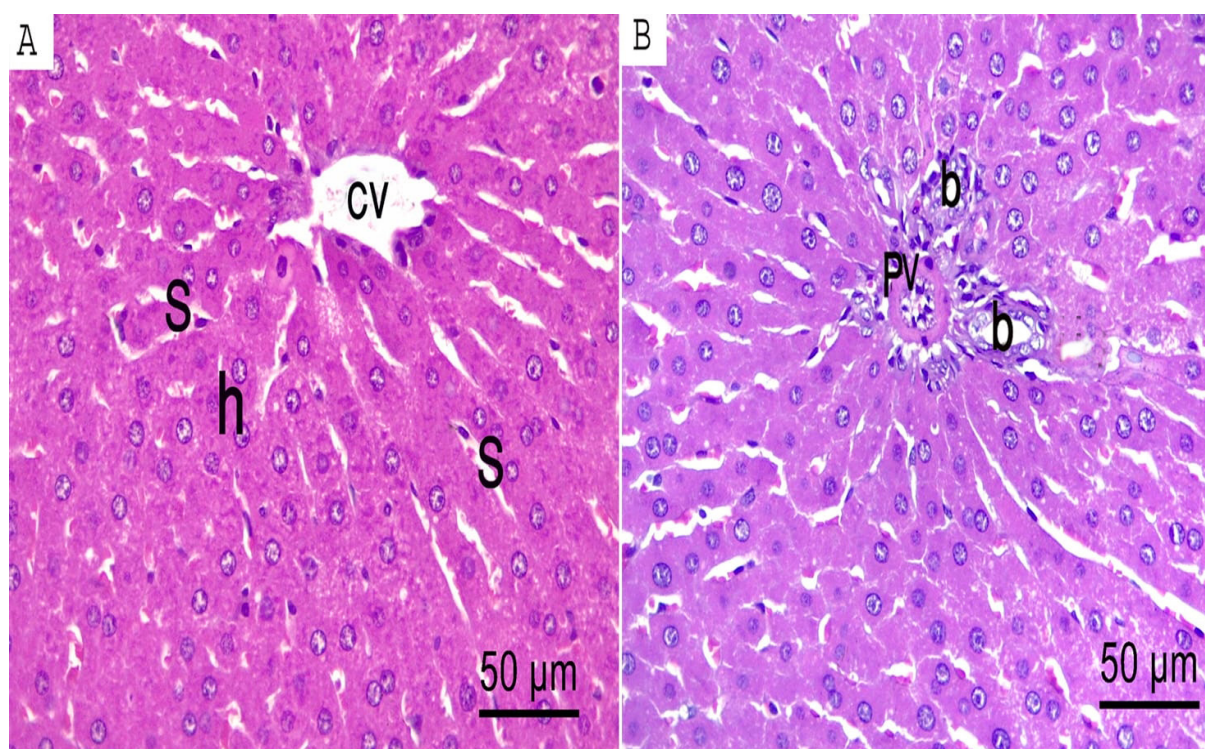


Fig. 4: Photomicrographs of H&E-stained liver sections of the control group, showing: (A) Central vein (CV) is surrounded by polygonal hepatocytes (h) with acidophilic cytoplasm and rounded vesicular nuclei. Narrow radiating blood sinusoids (S) are observed. (B) Portal triad containing portal venule (PV), and bile ductule (b). (H & E x 400)

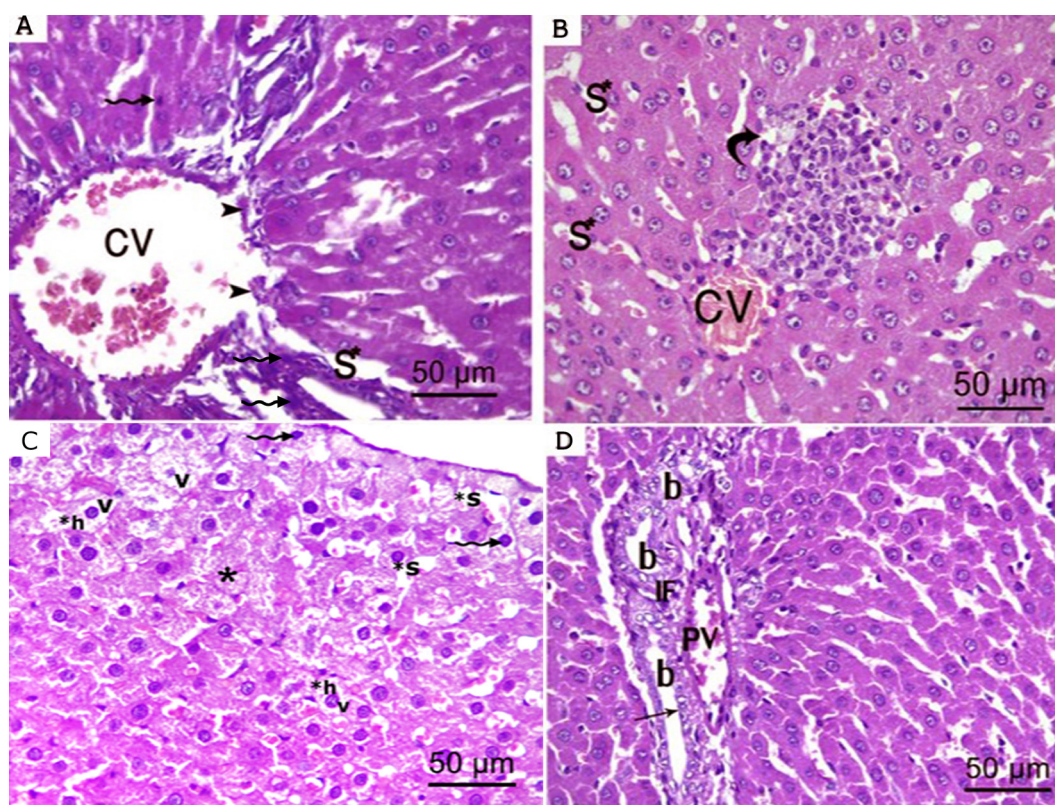


Fig. 5: Photomicrographs of H&E-stained liver sections of PFOS-treated group, showing: (A) Dilated congested central vein (CV) with partial detachment of its endothelium (arrowheads), and dilated blood sinusoid (S*). Darkly stained nuclei of hepatocytes (zigzag arrow) are observed. (B) A focus of mononuclear cellular infiltration (curved arrow) close to congested central vein (CV), and congested blood sinusoids (S*) are observed. (C) Some hepatocytes with ballooning (h*), and vacuolated cytoplasm (V) are seen. Darkly stained shrunken nuclei of some hepatocytes (zigzag arrows) are seen. Area of hepatocytes lost their nuclei (star) and dilated congested blood sinusoids (S*) are also seen. (D) Dilated congested portal venule (PV), mononuclear cellular infiltration (IF), multiple dilated bile ductules (b), and stratification of bile ductular epithelium (arrow) are also seen. (H & E x 400)

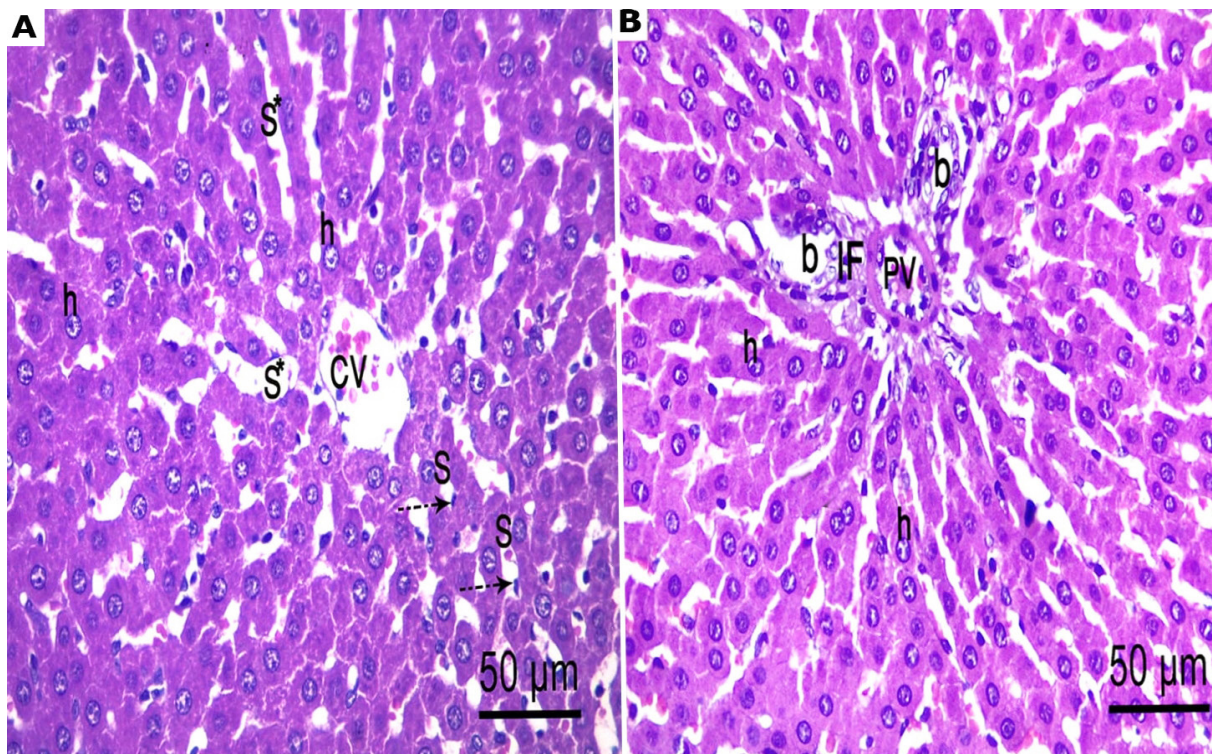


Fig. 6: Photomicrographs of H&E-stained liver sections of PFOS+QE group, showing: (A) Central vein (CV) is surrounded by hepatocytes with vesicular nuclei and acidophilic cytoplasm (h). Some sinusoids are apparently normal (S), and the endothelial lining (interrupted arrow) is seen, but other sinusoids are still dilated (S*). (B) Portal venule (PV) and bile ductules (b) are apparently normal. Some inflammatory cells are seen (IF). Most hepatocytes have acidophilic cytoplasm and vesicular nuclei (h). (H & E x 400)

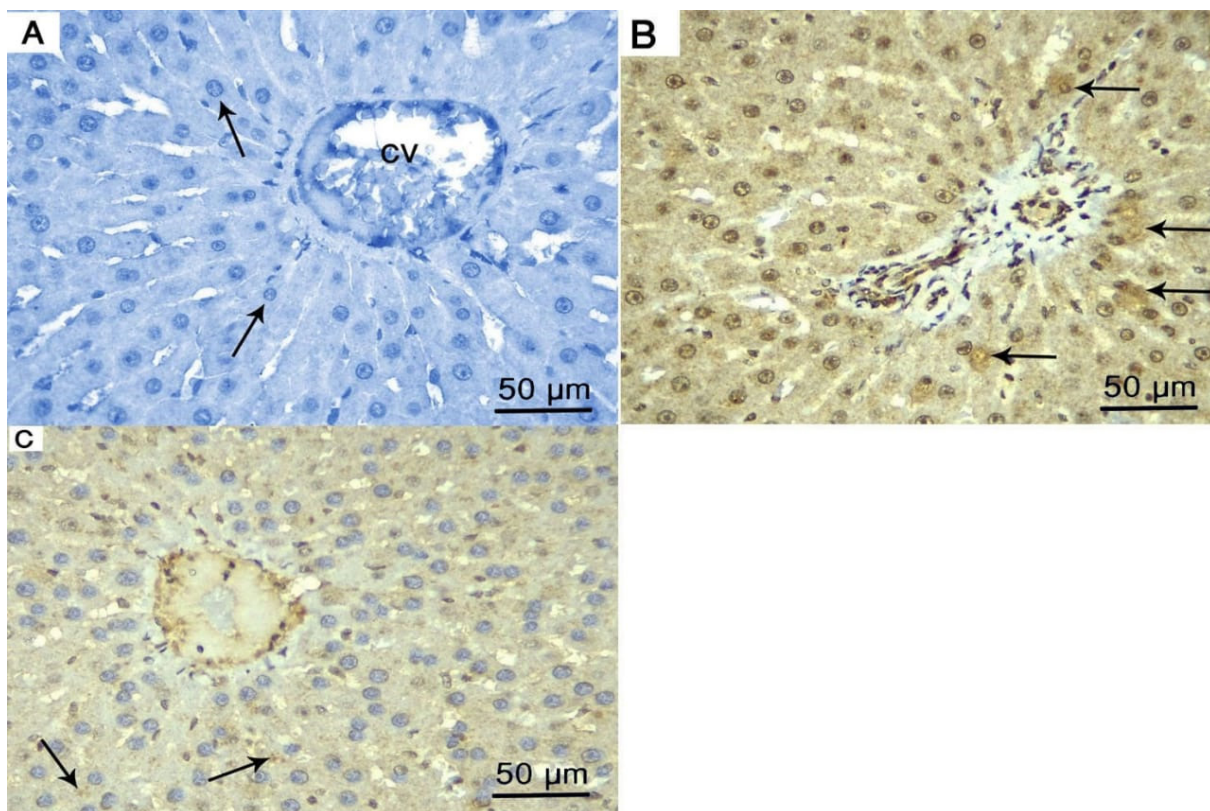


Fig. 7: Photomicrographs of sections in the liver of Caspase-3 immune reaction showing: (A) The control group, central vein (CV), is surrounded by negative immune reactions in the cytoplasm of the hepatocytes (arrows). (B) PFOS-treated group with strong positive immune reaction in the hepatocyte's cytoplasm (arrows). (C) PFOS+QE group with moderate positive immune reactions in the hepatocyte's cytoplasm (arrows). (Immunoperoxidase technique for caspase3 X 400)

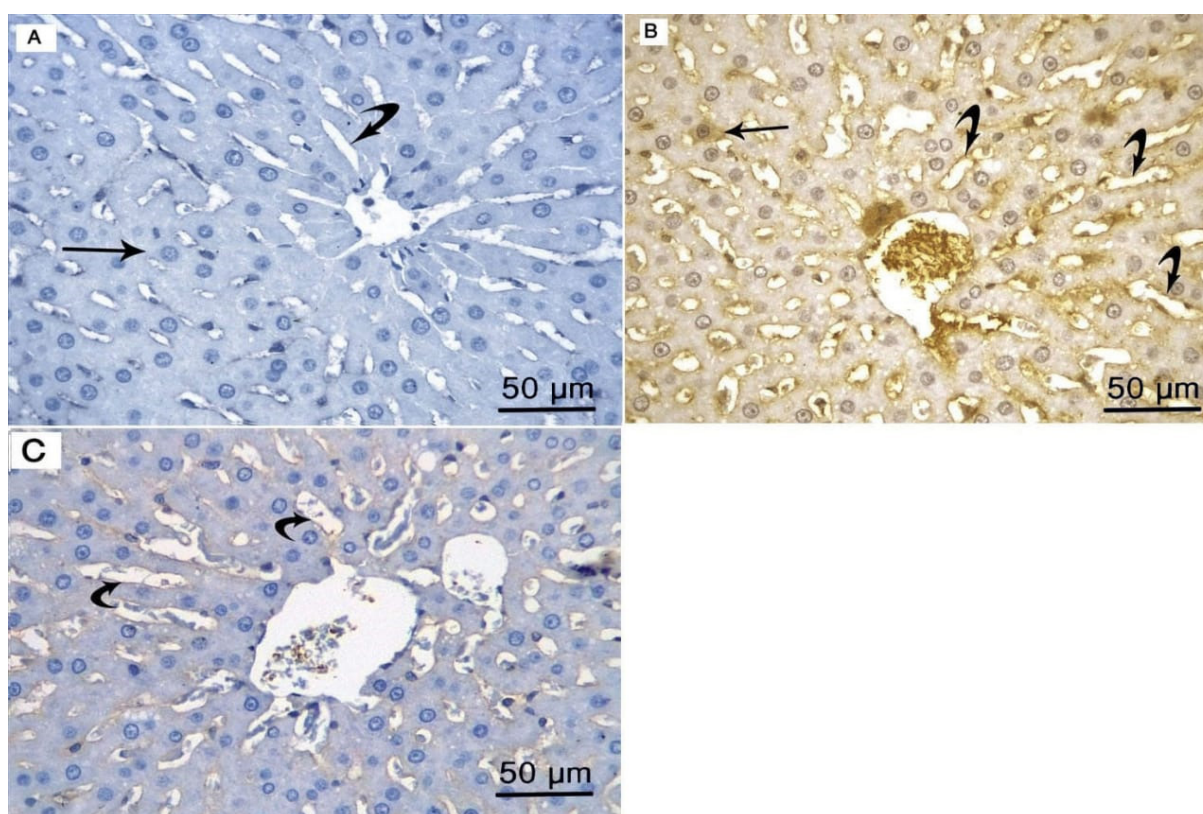


Fig. 8: Photomicrographs of sections in the liver of TNF- α immune reaction showing: (A) The control group with negative immunoreactions in the hepatocyte's cytoplasm (arrow) and in the wall of sinusoids (curved arrow). (B) PFOS-treated group with strong positive immune reactions in the hepatocyte's cytoplasm (arrow) and in the wall of sinusoids (curved arrows). (C) PFOS+QE group with moderate positive immune reactions in the wall of sinusoids (curved arrows). (Immunoperoxidase technique for TNF- α X 400)

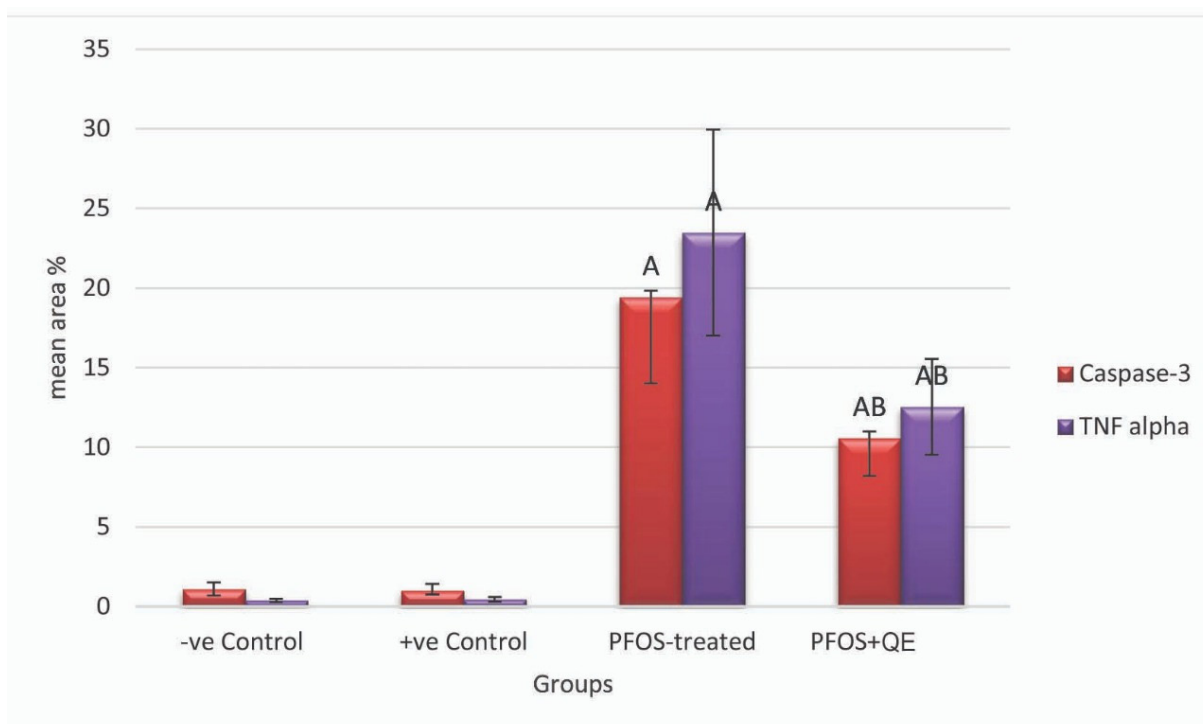


Fig. 9: Histogram showing comparison of mean area percentage of caspase-3 and TNF- α immunostaining among different studied groups. A highly significant difference with control groups ($P < 0.001$). B highly significant difference with the PFOS-treated group ($P < 0.001$).

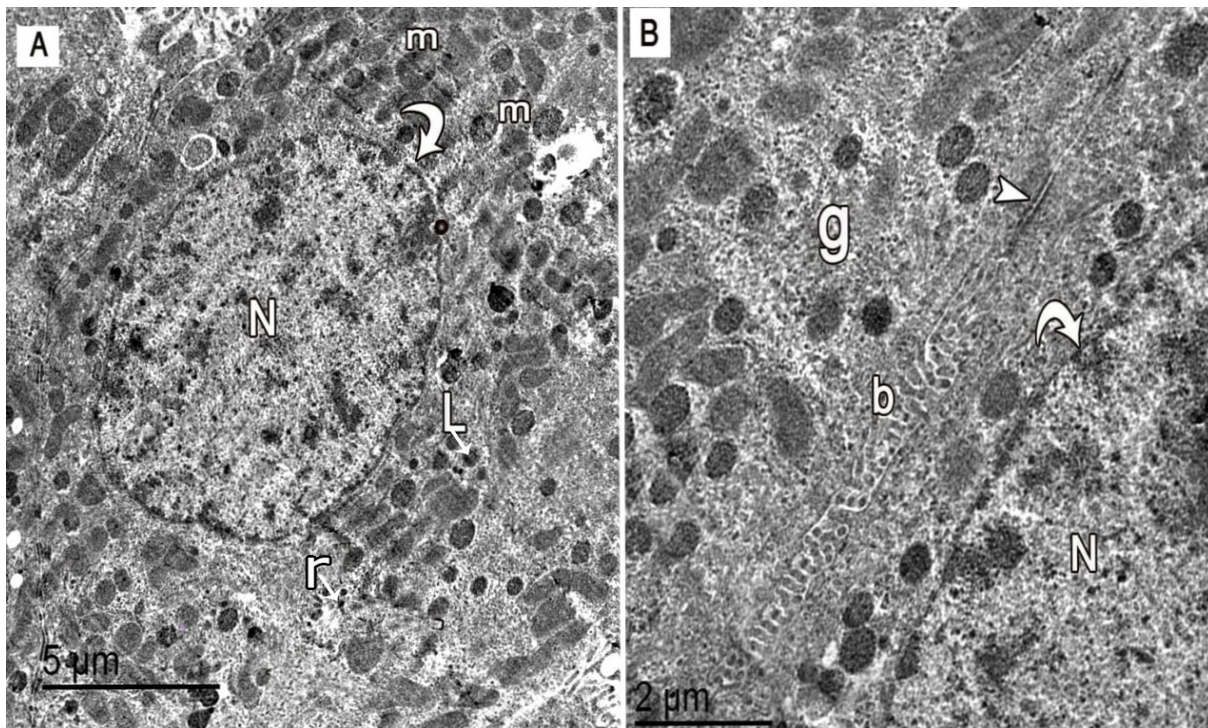


Fig. 10: Electron micrographs of sections in the liver of control group, showing: (A) A normal hepatocyte with an euchromatic nucleus (N) and intact regular nuclear membrane (curved arrow). Its cytoplasm has numerous mitochondria (m), ribosomes (r), and lysosomes (L). (B) Higher magnification of a normal hepatocyte with an euchromatic nucleus (N) and intact nuclear membrane (curved arrow). Bile canaliculus (b) with microvilli projecting into or occupying its lumen, glycogen granules (g) and normal cell to cell junction (arrowhead) are also seen. TEM Scale bar = A- 5 microns x1500 and, B- 2 microns x2000.

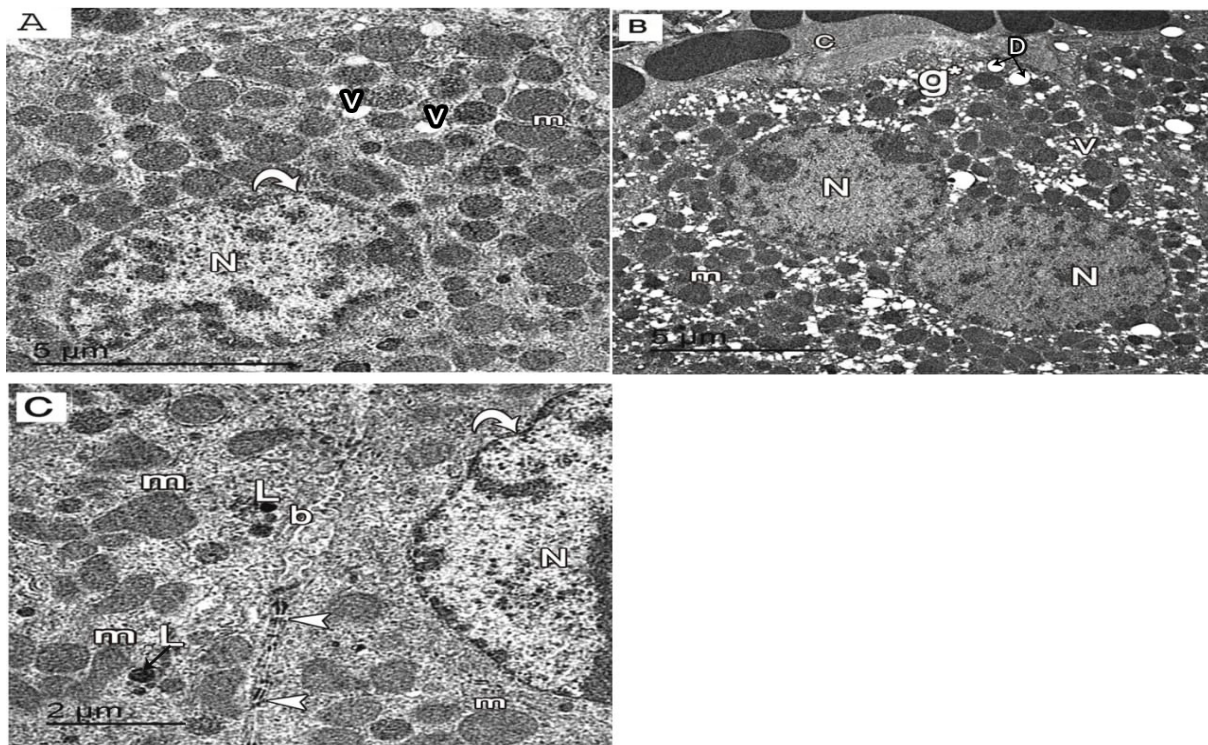


Fig. 11: Electron micrographs of sections in the liver of PFOS-treated group, showing: (A) A hepatocyte with heterochromatic nucleus (N) and irregular nuclear membrane (curved arrow). The cytoplasm holds multiple swollen mitochondria (m). Some cytoplasmic vacuoles (V) are also seen. (B) A binucleated hepatocyte with heterochromatic (N) and extensive vacuolations (V). Its cytoplasm also has multiple disrupted mitochondria (m) and some lipid droplets (D). The cell boundary of the hepatocyte shows area of collagen deposits (C). Depletion of glycogen granules (g*) is also seen. (C) A higher magnification of a hepatocyte showing nucleus (N) with irregular nuclear membrane (curved arrow). Its cytoplasm holds swollen and abnormally shaped mitochondria (m). Some lysosomes (L) are seen. Bile canaliculus (b) with dilated lumen and tight cell to cell junctions (arrow heads) are still seen. TEM Scale bar = A- 5 microns x 1000 and, C-2 microns x 2000.

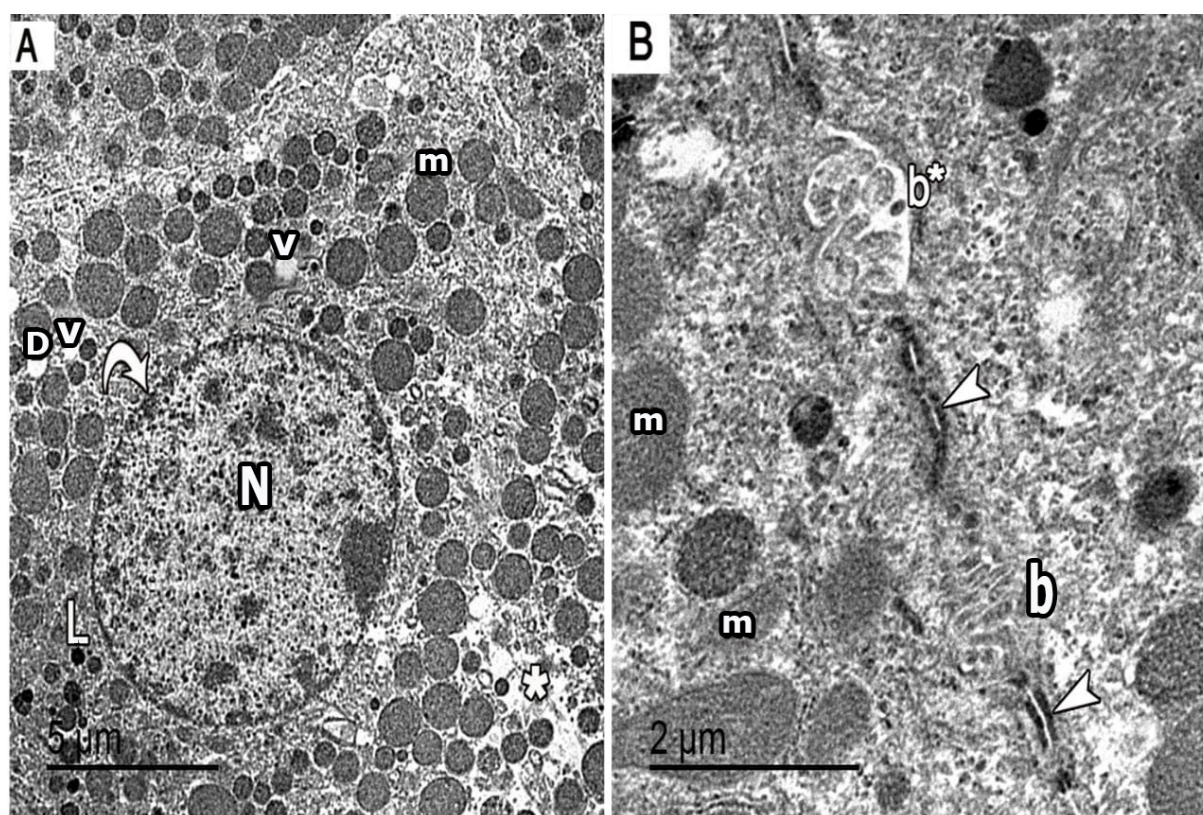


Fig. 12: Electron micrographs of sections in the liver of the PFOS+QE group, showing: (A) An apparently normal hepatocyte with rounded euchromatic nucleus (N) and intact nuclear membrane (curved arrow). Its cytoplasm holds numerous rounded mitochondria (m) and some lysosomes (L). Rarefied area of the cytoplasm is still present (star) with some vacuolations (V) are still seen in the cytoplasm. (B) Two bile canaliculi are seen, one of them has microvilli occupying its lumen (b), and the other has degenerated microvilli and wide lumen (b*). The surrounding mitochondria (m) are apparently normal. Tight Cell to cell junctions (arrow heads) are still seen. TEM Scale bar = A- 5 microns x1000 and, B- 2 microns x3000.

DISCUSSION

Perfluoroalkyl substances are environmentally persistent and bio accumulative chemicals, including PFOS and PFOA. Perfluorooctane sulfonate (PFOS) has caused great health concerns due to its ubiquitous environmental distribution and its long half-life in animals and humans^[45]. Quercetin possesses a broad spectrum of pharmacological properties, comprising anti-oxidant, anti-inflammatory, as well as cytoprotective properties^[46].

As a result, great focus has indeed been paid in this work to explore the mechanisms of toxicity of PFOS, on the liver, since the accessible toxicological information on the harmful impact of this environmental toxin remains inadequate and also to explore the effectiveness of QE against PFOS-induced hepatic toxicity.

Bodyweight is often the most sensitive predictor of toxicant deleterious effects^[47]. Also, the notion that liver enlargement was indeed a sensitive indication of PFOS poisoning was perpetuated^[48-50].

In the present study, there was a significant decrease in body weights (BW) of rats treated with PFOS. Additionally, there was a significant increase in liver weights as well as relative liver weights in the PFOS-treated group compared to those of the control and PFOS+QE groups. Such findings supported those of Wan *et al.* (2012)^[48]; Kim *et al.*^[51], who

explained that increased liver weight is related to increases of cell size, cell number, and cell replication.

In biochemical tests, liver damage was reflected by the level of AST and ALT^[52]. In the current work, the significantly increased ALT, AST, and ALP levels in the PFOS-treated group suggested its hepatic toxicological effect. This result was agreed with Jin *et al.*^[53], who established an association between PFAS-induced liver injury and elevated ALT, AST levels. Quercetin could significantly decrease the liver enzymes in rats exposed to PFOS. These results agreed with Zou *et al.* (2015)^[31], who reported that QE was able to normalize the levels of ALT, AST, ALP, Lactate dehydrogenase (LDH), and total bile acid (TBA).

Oxidative stress is primarily caused by an imbalance in the generation of reactive oxygen species (ROS) and the anti-oxidative defense mechanisms of the cell, in which ROS production exceeds the anti-oxidant capacity of the cell. Superoxide dismutase (SOD) and CAT are the most critical anti-oxidative enzymes that can eliminate ROS accumulation in a short time^[54].

Lipid peroxidation is considered the most important and detrimental cellular consequence of free radicals. Malondialdehyde (MDA) is a by-product of the lipid peroxidation process and one of the most common aldehyde derivatives^[55]. Malondialdehyde (MDA) is a biomarker of oxidative damage^[56,57].

Perfluorooctane sulfonate (PFOS) induced ROS accumulation by decreasing anti-oxidant enzyme activities in the present work. So, hepatic toxicity was suggested to be mediated via oxidative stress. This was evident by the current data, which found that SOD, GPX, and CAT activities significantly decreased. At the same time, MDA was significantly increased in the PFOS-treated group compared to the control and PFOS+QE groups. These results agreed with Wielsøe *et al.*^[58], who stated that PFAS induced an imbalance of the cellular redox homeostasis, which has been reported as a possible mechanism of action. Significantly, QE exhibited anti-oxidant effects in rats exposed to PFOS, evidenced by enhanced SOD, GPX, and CAT levels and prevented MDA accumulation. The anti-oxidant activities of QE have been attributed to direct free radical scavenging effects^[59] and inhibition of lipid peroxidation^[60].

In the current study, the PFOS-treated group presented a significant increase in area percentage of immunoreactivity of Caspase 3. Numerous studies have established that oxidative stress could induce apoptosis via various pathways^[61-63]. Excessive ROS production results in mitochondrial dysfunction, which manifests as a decrease in the mitochondria membrane potential, the release of Cyt-C into the cytosol, and activation of caspase9 and 3, eventually initiating apoptotic activity^[64,65].

Moreover, the present work indicated that QE significantly ameliorated apoptotic activity of PFOS, evident by a significant decrease in area percentage of immunoreactivity of caspase3 in the PFOS+QE group compared to PFOS treated group. This finding agreed with those of Chao *et al.* (2009)^[66] and Kim *et al.* (2009)^[67], who clarified that QE could inhibit apoptosis by changing the expression of caspase-3, Bcl-2, and Bax.

Reactive oxygen species (ROS) are inflammatory mediators^[68]. Tumor Necrotic Factor Alpha (TNF- α) has closely participated in inflammatory stress. The role of inflammatory changes induced by PFOS in the liver had been presented in our study by the significant increase in area percentage of immunoreactivity of TNF- α in the PFOS-treated group. This finding agreed with Han *et al.*^[69], who reported that TNF- α activated the NF- κ B signaling pathway, led to the secretion of inflammatory factors such as IL-1 β or IL-6, which further aggravated liver inflammation. Fouad *et al.*^[70] added that TNF- α could induce apoptosis in liver cells through caspase 3 activation upon binding to its receptor.

Quercetin significantly displayed a role against PFOS induced inflammatory changes evident by the significantly decreased area percentage of immunoreactivity of TNF- α in the PFOS+QE group compared to the PFOS group. This is compatible with QE's established anti-inflammatory properties^[23], including inhibiting pro-inflammatory cytokines such as IL-6, IL-8, TNF- and activating NF- κ B and other pathways^[71].

C-reactive protein (CRP) is a marker of inflammation produced pre-dominately by the liver^[72]. In the present study, exposure to PFOS significantly increased the levels of CRP in the hepatic tissue. This result agreed with Yang *et al.*^[73]. However, QE could significantly ameliorate CRP levels in rats exposed to PFOS. These results agreed with Zou *et al.* (2015)^[31] who explained that QE administration to mice treated with PFOA led to the decline in the pro-inflammatory cytokines (interleukin 6, cyclooxygenase 2) and CRP levels.

Histopathological assessments are regularly used for identifying organ changes related to chemical exposure. Reactive oxygen species (ROS) derived damage to natural and structured cellular components is generally considered a serious mechanism in histological disorders^[74].

In the current work, H&E-stained sections of the liver tissue of the PFOS-treated group further confirmed the PFOS-induced hepatic damage where there were dilated congested central and portal veins. Some blood sinusoids were dilated and congested. Hu *et al.* (2013)^[75], reported that portal hypertension is the reason for the congestion and dilatation of central and portal veins. On the other hand, Puche *et al.*, (2013)^[76], attributed sinusoidal dilatation to the activation of perisinusoidal cells which had contractile properties.

Some hepatic lobules showed focus of mononuclear cellular infiltration close to the congested central vein. Rahman & Macnee, (2000)^[77], stated that the inflammatory cellular infiltration around portal and central veins was related to oxidative stress that resulted in generation of mediators such as IL-8 and cytokine-induced neutrophil chemoattractant which attracts the inflammatory cells into microcirculation and then to the liver interstitium due to destruction of the endothelial cells by the free radicals.

Some hepatocytes were with ballooning, and vacuolated cytoplasm. These findings were in accordance with Seacat *et al.*, (2003)^[78], who reported that the hepatocytes showed swelling and vacuolization. Izabela *et al.*, (2011)^[79], suggested that vacuolated cells may be macrophages containing many lipid droplets (foam cells). They added that the increased levels of ROS cause oxidative modification of low-density lipoproteins (LDLs) and formation of oxidized form (ox-LDLs) which are internalized by the macrophages and is implicated in the formation of foam cells.

In the current study some other hepatocytes were with darkly stained shrunken nuclei. This finding was in accordance with Taylor *et al.*, (2008)^[80], who stated that hyperchromatic nuclei were a degenerative change denoting apoptosis.

Additionally, in the present study there were multiple dilated bile ductules, and stratification of bile ductular epithelium. Roskams *et al.* (2004)^[81] and Alvaro *et al.* (2007)^[82] proposed that cellular changes in the epithelium of bile ductules may contribute to the activation of hepatic

stem/progenitor cells, the proliferation of preexisting cholangiocytes, or ductular metaplasia of mature hepatocytes.

In the current work, H&E-stained sections of the liver tissue of the PFOS+QE group showed improvement in liver architecture. These findings agreed with Mostafavi-Pour *et al.* (2008)^[83] and Yousef *et al.* (2010)^[84], who reported that QE has a powerful ameliorative effect in the hepatic structure damaged by some agents as cadmium and cyclosporine A. Padma *et al.* (2012)^[85] attributed the efficacy of QE as a potent anti-oxidant activity.

In the current work, electron microscope examination of hepatocytes of the PFOS-treated group confirmed the hepatic toxicity of PFOS. There were abnormal shaped hepatocytic nuclei with irregular nuclear membrane. These findings were in accordance with Chowdhury *et al.*, (2006)^[86] who attributed those changes of the nuclear and cellular outlines with cell shrinkage as morphological features of apoptosis, which is a pathological or accidental mode of cell death and is ATP independent.

There were numerous dilated abnormally shaped mitochondria. Malondialdehyde (MDA) triggers mitochondrial damage via increasing ROS production and modulating the expression of mitochondrial proteins^[87,88]. Kao *et al.* (2004)^[89], established a link between mitochondrial swelling and alterations in the Ca-ATPase activity and calcium content of the mitochondria, which result in a disruption of calcium homeostasis. Additionally, almost the same authors noted that inhibiting Na/K ATPase (the energy-dependent pump in the plasma membrane) results in intracellular sodium accumulation and osmotic gain of water, resulting in mitochondrial swelling. The results of our study revealed a considerable increase in ROS and MDA concentrations as a result of PFOS administration, signifying a deterioration in the structural and functional integrity of the mitochondrial membrane.

Kulisz *et al.*^[90] and Tokunaga *et al.*^[91] directly attributed hepatocyte vacuolation noticed in the present study to the release of free radicals, which enhance the discharge of lysosomal enzymes into the cytoplasm and subsequent oxidation of the cellular protein architecture, leading to protein fragmentation

In this work, electron microscope examination of PFOS+QE group showed some improvement of hepatocytes ultrastructure compared with that of PFOS exposed group. Chen (2010)^[92], reported that QE effectively ameliorated hepatic ultrastructural changes, producing a satisfactory hepatoprotective effect against ethanol toxicity. Quercetin has been shown to alter mitochondrial biogenesis, eliminate excessive mt ROS, and preserve membrane potential in order to influence mitochondrial function^[93].

Additionally, electron microscope examination of the PFOS+QE group showed some bile canaliculi contained microvilli that occupy its lumen while other bile canaliculi had degenerated microvilli and wide lumen. This result

agreed with that of Peres *et al.* (2000)^[94], who reported that QE treatment resulted in a reduction in liver oxidative stress, the proliferation of bile ducts, and fibrosis in biliary obstructed rats, so it could be used to preserve liver function in biliary obstruction.

CONCLUSION

From the findings of this study, it was concluded that oral supplementation of PFOS (20 mg/kg/day) for 28 days could cause hepatotoxicity. This study demonstrated the mechanism of action of PFOS-induced hepatic injury through preventing anti-oxidant enzyme activities, hence triggering apoptosis and inflammation. Oxidative stress caused detrimental changes in the histological structure of the liver at the level of light and electron microscope. Administration of QE simultaneously with PFOS caused moderate alleviation of the alterations associated with PFOS administration. To our experience and understanding, this work is the first to demonstrate QE's capacity to mitigate PFOS-induced liver damage in rodents. This is mainly due to its antioxidant, anti-inflammatory, as well as anti-apoptotic properties.

FUNDING

This work did not receive any funding from funding organizations in the public, commercial, or not-for-profit sectors. However, Ministry of high education and Scientific Research partially supported this work by providing the required tools and chemicals.

ABBREVIATIONS

PFOS: Perfluorooctane sulfonate, **PFASs:** Perfluoroalkyl substances, **QE:** Quercetin, **CAT:** Catalase, **ALT:** Alanine aminotransferase, **ALP:** Alkaline phosphatase, **AST:** Aspartate aminotransferase, **SOD:** superoxide dismutase, **GPX:** glutathione peroxidase, **CRP:** C reactive protein, **MDA:** malondialdehyde, **PFOA:** Perfluorooctanoic acid, **POPs:** persistent organic pollutants class, **LDH:** Lactate dehydrogenase, **TBA:** total bile acid, **ROS:** reactive oxygen species.

CONFLICT OF INTERESTS

There are no conflicts of interest.

REFERENCES

1. Byrne S, Seguinot-Medina S, Miller P, *et al.* Exposure to polybrominated diphenyl ethers and perfluoroalkyl substances in a remote population of Alaska Natives. *Environ Pollut.* 2017;231(Pt 1):387-395.
2. Nian M, Li QQ, Bloom M, *et al.* Liver function biomarkers disorder is associated with exposure to perfluoroalkyl acids in adults: Isomers of C8 Health Project in China. *Environ Res.* 2019;172:81-88.
3. Blake BE, Fenton SE. Early life exposure to per- and polyfluoroalkyl substances (PFAS) and latent health outcomes: A review including the placenta as a target tissue and possible driver of peri- and postnatal effects. *Toxicology.* 2020;443:152565.

4. Lee JW, Lee JW, Kim K, *et al.* PFOA-induced metabolism disturbance and multi-generational reproductive toxicity in *Oryzias latipes*. *J Hazard Mater.* 2017;340:231-240.
5. Bach CC, Bech BH, Brix N, Nohr EA, Bonde JP, Henriksen TB. Perfluoroalkyl and polyfluoroalkyl substances and human fetal growth: a systematic review. *Crit Rev Toxicol.* 2015;45(1):53-67.
6. Cui Q, Shi F, Pan Y, Zhang H, Dai J. Per- and polyfluoroalkyl substances (PFASs) in the blood of two colobine monkey species from China: Occurrence and exposure pathways. *Sci Total Environ.* 2019;674:524-531.
7. de la Torre A, Navarro I, Sanz P, Martínez MLÁ. Occurrence and human exposure assessment of perfluorinated substances in house dust from three European countries. *Sci Total Environ.* 2019;685:308-314.
8. Chou WC, Lin Z. Bayesian evaluation of a physiologically based pharmacokinetic (PBPK) model for perfluorooctane sulfonate (PFOS) to characterize the interspecies uncertainty between mice, rats, monkeys, and humans: Development and performance verification. *Environ Int.* 2019;129:408-422.
9. Dourson ML, Gadagbui B, Onyema C, McGinnis PM, York RG. Data derived Extrapolation Factors for developmental toxicity: A preliminary research case study with perfluorooctanoate (PFOA). *Regul Toxicol Pharmacol.* 2019;108:104446.
10. Domazet SL, Jensen TK, Wedderkopp N, Nielsen F, Andersen LB, Grøntved A. Exposure to perfluoroalkylated substances (PFAS) in relation to fitness, physical activity, and adipokine levels in childhood: The European Youth Heart Study. *Environ Res.* 2020;191:110110.
11. Ericson I, Domingo JL, Nadal M, *et al.* Levels of perfluorinated chemicals in municipal drinking water from Catalonia, Spain: public health implications. *Arch Environ Contam Toxicol.* 2009;57(4):631-638.
12. Tian Z, Kim SK, Shoeib M, Oh JE, Park JE. Human exposure to per- and polyfluoroalkyl substances (PFASs) via house dust in Korea: Implication to exposure pathway. *Sci Total Environ.* 2016;553:266-275.
13. Grandjean P, Heilmann C, Weihe P, *et al.* Estimated exposures to perfluorinated compounds in infancy predict attenuated vaccine antibody concentrations at age 5-years. *J Immunotoxicol.* 2017;14(1):188-195.
14. Rovira J, Martínez MÁ, Sharma RP, *et al.* Prenatal exposure to PFOS and PFOA in a pregnant women cohort of Catalonia, Spain. *Environ Res.* 2019;175:384-392.
15. Augustsson A, Lennqvist T, Osbeck CMG, *et al.* Consumption of freshwater fish: A variable but significant risk factor for PFOS exposure. *Environ Res.* 2021;192:110284.
16. Tohge T, de Souza LP, Fernie AR. Current understanding of the pathways of flavonoid biosynthesis in model and crop plants [published correction appears in *J Exp Bot.* 2018 Aug 14;69(18):4497]. *J Exp Bot.* 2017;68(15):4013-4028.
17. Elkady MA, Shalaby S, Fathi F, El-Mandouh S. Effects of quercetin and rosuvastatin each alone or in combination on cyclophosphamide-induced premature ovarian failure in female albino mice. *Hum Exp Toxicol.* 2019;38(11):1283-1295.
18. Jakaria M, Azam S, Jo SH, Kim IS, Dash R, Choi DK. Potential Therapeutic Targets of Quercetin and Its Derivatives: Its Role in the Therapy of Cognitive Impairment. *J Clin Med.* 2019;8(11):1789.
19. Magar RT, Sohng JK. A Review on Structure, Modifications and Structure-Activity Relation of Quercetin and Its Derivatives. *J Microbiol Biotechnol.* 2020;30(1):11-20.
20. Alidadi H, Khorsandi L, Shirani M. Effects of Quercetin on Tubular Cell Apoptosis and Kidney Damage in Rats Induced by Titanium Dioxide Nanoparticles. *Malays J Med Sci.* 2018;25(2):72-81.
21. Moujahed S, Ruiz A, Hallegue D, Sakly M. Quercetin alleviates styrene oxide-induced cytotoxicity in cortical neurons *in vitro* via modulation of oxidative stress and apoptosis [published online ahead of print, 2020 Dec 9]. *Drug Chem Toxicol.* 2020;1-10.
22. Wang G, Li Y, Lei C, *et al.* Quercetin exerts antidepressant and cardioprotective effects in estrogen receptor α -deficient female mice via BDNF-AKT/ERK1/2 signaling. *J Steroid Biochem Mol Biol.* 2021;206:105795.
23. Li Y, Yao J, Han C, *et al.* Quercetin, Inflammation and Immunity. *Nutrients.* 2016;8(3):167.
24. Wang S, Yao J, Zhou B, *et al.* Bacteriostatic Effect of Quercetin as an Antibiotic Alternative *In Vivo* and Its Antibacterial Mechanism *In Vitro*. *J Food Prot.* 2018;81(1):68-78.
25. Dong Y, Lei J, Zhang B. Effects of dietary quercetin on the antioxidative status and cecal microbiota in broiler chickens fed with oxidized oil. *Poult Sci.* 2020;99(10):4892-4903.
26. Ozyel B, Le Gall G, Needs PW, Kroon PA. Anti-Inflammatory Effects of Quercetin on High-Glucose and Pro-Inflammatory Cytokine Challenged Vascular Endothelial Cell Metabolism. *Mol Nutr Food Res.* 2021;65(6):e2000777.

27. Lin W, Wu Y, Wang J, *et al.* Network Pharmacology Study of the Hepatoprotective Effects of Quercetin-Containing Traditional Chinese Medicine, *Anoectochilus roxburghii*, and Validation of Quercetin as an Anti-Liver Injury Agent in a Mouse Model of Liver Injury. *Med Sci Monit.* 2020;26:e923533.
28. Razali N, Abdul Aziz A, Lim CY, Mat Junit S. Investigation into the effects of antioxidant-rich extract of *Tamarindus indica* leaf on antioxidant enzyme activities, oxidative stress and gene expression profiles in HepG2 cells. *PeerJ.* 2015;3:e1292. Published 2015 Oct 1.
29. Sun X, Yamasaki M, Katsube T, Shiwaku K. Effects of quercetin derivatives from mulberry leaves: Improved gene expression related hepatic lipid and glucose metabolism in short-term high-fat fed mice. *Nutr Res Pract.*
30. Miltonprabu S, Tomczyk M, Skalicka-Woźniak K, *et al.* Hepatoprotective effect of quercetin: From chemistry to medicine. *Food Chem Toxicol.* 2017;108(Pt B):365-374.
31. Srinivasan, P., Vijayakumar, S., Kothandaraman, S., & Palani, M. (2018). Anti-diabetic activity of quercetin extracted from *Phyllanthus emblica* L. fruit: In silico and in *vivo* approaches. *Journal of pharmaceutical analysis*, 8(2), 109-118.
32. Cui L, Zhou QF, Liao CY, Fu JJ, Jiang GB. Studies on the toxicological effects of PFOA and PFOS on rats using histological observation and chemical analysis. *Arch Environ Contam Toxicol.* 2009;56(2):338-349.
33. Vogler, G. A. Anesthesia and analgesia. In *The laboratory rat*, 2006: 627-664. Academic Press.
34. REITMAN S, FRANKEL S. A colorimetric method for the determination of serum glutamic oxalacetic and glutamic pyruvic transaminases. *Am J Clin Pathol.* 1957;28(1):56-63.
35. LOWRY OH, ROSEBROUGH NJ, FARR AL, RANDALL RJ. Protein measurement with the Folin phenol reagent. *J Biol Chem.* 1951;193(1):265-275.
36. Bradford MM. A rapid and sensitive method for the quantitation of microgram quantities of protein utilizing the principle of protein-dye binding. *Anal Biochem.* 1976;72:248-254.
37. Minami M, Yoshikawa H. A simplified assay method of superoxide dismutase activity for clinical use. *Clin Chim Acta.* 1979;92(3):337-342.
38. Paglia DE, Valentine WN. Studies on the quantitative and qualitative characterization of erythrocyte glutathione peroxidase. *J Lab Clin Med.* 1967;70(1):158-169.
39. Aebi H. Catalase in *vitro*. *Methods Enzymol.* 1984;105:121-126.
40. Satoh K. Serum lipid peroxide in cerebrovascular disorders determined by a new colorimetric method. *Clin Chim Acta.* 1978;90(1):37-43.
41. Bancroft JD, Layton C. The hematoxylin and eosin. In: Suvarna KS, Layton C, Bancroft JD (ed.) *Bancroft's Theory and Practice of Histological Techniques E-Book*. 8th ed. Elsevier Health Sciences. 2018; Ch:10, Pp 126–138.
42. Ramos-Vara JA. Principles and Methods of Immunohistochemistry. *Methods Mol Biol.* 2017;1641:115-128.
43. Glauert, Audrey M, and Peter R. Lewis. *Biological Specimen Preparation for Transmission Electron Microscopy*. Princeton: Princeton University Press, 2014.
44. Stehlik-Barry K, Babinec AJ. Comparing Means and ANOVA. In: *Data Analysis with IBM SPSS Statistics*, Packt Publishing Ltd. 2017; Ch:11, pp 229–265.
45. Wan C, Han R, Liu L, *et al.* Role of miR-155 in fluorooctane sulfonate-induced oxidative hepatic damage via the Nrf2-dependent pathway. *Toxicol Appl Pharmacol.* 2016;295:85-93.
46. Wang W, Sun C, Mao L, *et al.* The biological activities, chemical stability, metabolism and delivery systems of quercetin: A review. *Trends Food Sci Technol.* 2016;56:21-38.
47. Salih NA, Al-Baggou BK. Effect of memantine hydrochloride on cisplatin-induced neurobehavioral toxicity in mice. *Acta Neurol Belg.* 2020;120(1):71-82.
48. Wan HT, Zhao YG, Wei X, Hui KY, Giesy JP, Wong CK. PFOS-induced hepatic steatosis, the mechanistic actions on β -oxidation and lipid transport. *Biochim Biophys Acta.* 2012;1820(7):1092-1101.
49. Case MT, York RG, Christian MS. Rat and rabbit oral developmental toxicology studies with two perfluorinated compounds. *Int J Toxicol.* 2001;20(2):101-109.
50. Seacat AM, Thomford PJ, Hansen KJ, Olsen GW, Case MT, Butenhoff JL. Subchronic toxicity studies on perfluorooctanesulfonate potassium salt in cynomolgus monkeys. *Toxicol Sci.* 2002;68(1):249-264.
51. Kim HS, Jun Kwack S, Sik Han E, Seok Kang T, Hee Kim S, Young Han S. Induction of apoptosis and CYP4A1 expression in Sprague-Dawley rats exposed to low doses of perfluorooctane sulfonate. *J Toxicol Sci.* 2011;36(2):201-210.
52. Valva P, Ríos DA, De Matteo E, Preciado MV. Chronic hepatitis C virus infection: Serum biomarkers in predicting liver damage. *World J Gastroenterol.* 2016;22(4):1367-1381.

53. Jin R, McConnell R, Catherine C, *et al.* Perfluoroalkyl substances and severity of nonalcoholic fatty liver in Children: An untargeted metabolomics approach. *Environ Int.* 2020;134:105220.
54. Lushchak VI. Contaminant-induced oxidative stress in fish: a mechanistic approach. *Fish Physiol Biochem.* 2016;42(2):711-747.
55. Gandhi S, Abramov AY. Mechanism of oxidative stress in neurodegeneration. *Oxid Med Cell Longev.* 2012;2012:428010.
56. Ma J, Li X. Alteration in the cytokine levels and histopathological damage in common carp induced by glyphosate [published correction appears in *Chemosphere.* 2020 Apr;245:125878]. *Chemosphere.* 2015;128:293-298.
57. Zhang Z, Zheng Z, Cai J, *et al.* Effect of cadmium on oxidative stress and immune function of common carp (*Cyprinus carpio* L.) by transcriptome analysis. *Aquat Toxicol.* 2017;192:171-177.
58. Wielsøe M, Long M, Ghisari M, Bonefeld-Jørgensen EC. Perfluoroalkylated substances (PFAS) affect oxidative stress biomarkers *in vitro*. *Chemosphere.* 2015;129:239-245.
59. Wielsøe M, Long M, Ghisari M, Bonefeld-Jørgensen EC. Perfluoroalkylated substances (PFAS) affect oxidative stress biomarkers *in vitro*. *Chemosphere.* 2015;129:239-245.
60. Loke WM, Proudfoot JM, McKinley AJ, *et al.* Quercetin and its *in vivo* metabolites inhibit neutrophil-mediated low-density lipoprotein oxidation. *J Agric Food Chem.* 2008;56(10):3609-3615.
61. Guo J, Xing H, Chen M, Wang W, Zhang H, Xu S. H2S inhalation-induced energy metabolism disturbance is involved in LPS mediated hepatocyte apoptosis through mitochondrial pathway. *Sci Total Environ.* 2019;663:380-386.
62. Liu Q, Wang W, Zhang Y, Cui Y, Xu S, Li S. Bisphenol A regulates cytochrome P450 1B1 through miR-27b-3p and induces carp lymphocyte oxidative stress leading to apoptosis. *Fish Shellfish Immunol.* 2020;102:489-498.
63. Wang Y, Zhao H, Liu Y, *et al.* Environmentally relevant concentration of sulfamethoxazole-induced oxidative stress-cascaded damages in the intestine of grass carp and the therapeutic application of exogenous lycopene. *Environ Pollut.* 2021;274:116597.
64. Jiaxin S, Shengchen W, Yirong C, Shuting W, Shu L. Cadmium exposure induces apoptosis, inflammation and immunosuppression through CYPs activation and antioxidant dysfunction in common carp neutrophils. *Fish Shellfish Immunol.* 2020;99:284-290.
65. Zhang J, Li L, Peng Y, *et al.* Surface chemistry induces mitochondria-mediated apoptosis of breast cancer cells via PTEN/PI3K/AKT signaling pathway. *Biochim Biophys Acta Mol Cell Res.* 2018;1865(1):172-185.
66. Chao CL, Hou YC, Chao PD, Weng CS, Ho FM. The antioxidant effects of quercetin metabolites on the prevention of high glucose-induced apoptosis of human umbilical vein endothelial cells. *Br J Nutr.* 2009;101(8):1165-1170.
67. Kim BM, Choi YJ, Han Y, Yun YS, Hong SH. N,N-dimethyl phytosphingosine induces caspase-8-dependent cytochrome c release and apoptosis through ROS generation in human leukemia cells. *Toxicol Appl Pharmacol.* 2009;239(1):87-97.
68. Carullo G, Cappello AR, Frattaruolo L, Badolato M, Armentano B, Aiello F. Quercetin and derivatives: useful tools in inflammation and pain management. *Future Med Chem.*
69. Han R, Zhang F, Wan C, Liu L, Zhong Q, Ding W. Effect of perfluorooctane sulphonate-induced Kupffer cell activation on hepatocyte proliferation through the NF- κ B/TNF- α /IL-6-dependent pathway. *Chemosphere.* 2018;200:283-294.
70. Fouad D, Badr A, Attia HA. Hepatoprotective activity of raspberry ketone is mediated via inhibition of the NF- κ B/TNF- α /caspase axis and mitochondrial apoptosis in chemically induced acute liver injury. *Toxicol Res (Camb).* 2019;8(5):663-676.
71. Yang D, Wang T, Long M, Li P. Quercetin: Its Main Pharmacological Activity and Potential Application in Clinical Medicine. *Oxid Med Cell Longev.* 2020;2020:8825387.
72. Pathak A, Agrawal A. Evolution of C-Reactive Protein. *Front Immunol.* 2019;10:943.
73. Yang B, Zou W, Hu Z, *et al.* Involvement of oxidative stress and inflammation in liver injury caused by perfluorooctanoic acid exposure in mice. *Biomed Res Int.* 2014;2014:409837.
74. Sepici-Dinçel A, Çağlan Karasu Benli A, Selvi M, *et al.* Sublethal cyfluthrin toxicity to carp (*Cyprinus carpio* L.) fingerlings: biochemical, hematological, histopathological alterations. *Ecotoxicol Environ Saf.* 2009;72(5):1433-1439.
75. Hu LS, George J, Wang JH. Current concepts on the role of nitric oxide in portal hypertension. *World J Gastroenterol.* 2013;19(11):1707-1717.
76. Puche, J; Saiman, Y and Friedman, S. Hepatic Stellate Cells and Liver Fibrosis. *Compr Physiol.* 2013; 3: 1473-1492.
77. Rahman, I. and MacNee, W. Oxidative stress and regulation of glutathione in lung inflammation. *European Respiratory Journal.* 2000; 16(3): 534-554.

-
78. Seacat, A.M., Thomford, P.J., Hansen, K.J., Clemen, L.A., Eldridge, S.R., Elcombe, C.R., Butenhoff, J.L. Sub-chronic dietary toxicity of potassium per-fluorooctanesulfonate in rats. *Toxicology*. 2003; 183, 117e131.
79. Izabela, G.; Irena, B. B.; Aldona, S.; Marta, R, *et al.* fluoride effects on cholesterol influx and expression of the scavenger receptor cd36 in thp1 differentiated monocyte/macrophage cells. *Fluoride*, 2011; 44(3): 135–142.
80. Taylor, R.C.; Cullen, S.P. and Martin, S.J. Apoptosis: controlled demolition at the cellular level. *Nature reviews, Molecular cell biology*, 2008; 9(3):231-241.
81. Roskams TA, Theise ND, Balabaud C, *et al.* Nomenclature of the finer branches of the biliary tree: canals, ductules, and ductular reactions in human livers. *Hepatology*. 2004;39(6):1739-1745.
82. Alvaro D, Mancino MG, Glaser S, *et al.* Proliferating cholangiocytes: a neuroendocrine compartment in the diseased liver. *Gastroenterology*. 2007;132(1):415-431.
83. Mostafavi-Pour Z, Zal F, Monabati A, Vessal M. Protective effects of a combination of quercetin and vitamin E against cyclosporine A-induced oxidative stress and hepatotoxicity in rats. *Hepatol Res*. 2008;38(4):385-392.
84. Yousef MI, Omar SA, El-Guendi MI, Abdelmegid LA. Potential protective effects of quercetin and curcumin on paracetamol-induced histological changes, oxidative stress, impaired liver and kidney functions and haematotoxicity in rat. *Food Chem Toxicol*. 2010;48(11):3246-3261.
85. Padma VV, Lalitha G, Shirony NP, Baskaran R. Effect of quercetin against lindane induced alterations in the serum and hepatic tissue lipids in wistar rats. *Asian Pac J Trop Biomed*. 2012;2(11):910-915.
86. Chowdhury, I.; Tharakan, B. and Bhat, G. Current concepts in apoptosis: The physiological suicide program revisited. *Cellular & molecular biology letters*, 2006; 11:506-525.
87. Caldiroli A, Auxilia AM, Capuzzi E, Clerici M, Buoli M. Malondialdehyde and bipolar disorder: A short comprehensive review of available literature. *J Affect Disord*. 2020; 274:31-37.
88. Cui R, Zhang H, Guo X, Cui Q, Wang J, Dai J. Proteomic analysis of cell proliferation in a human hepatic cell line (HL-7702) induced by perfluorooctane sulfonate using iTRAQ. *J Hazard Mater*. 2015;299:361-370.
89. Kao WF, Deng JF, Chiang SC, *et al.* A simple, safe, and efficient way to treat severe fluoride poisoning—oral calcium or magnesium. *J Toxicol Clin Toxicol*. 2004;42(1):33-40.
90. Kulisz A, Chen N, Chandel NS, Shao Z, Schumacker PT. Mitochondrial ROS initiate phosphorylation of p38 MAP kinase during hypoxia in cardiomyocytes. *Am J Physiol Lung Cell Mol Physiol*. 2002;282(6):L1324-L1329.
91. Tokunaga T, Morshed SR, Otsuki S, *et al.* Effect of antioxidants, oxidants, metals and saliva on cytotoxicity induction by sodium fluoride. *Anticancer Res*. 2003;23(5A):3719-3726.
92. Chen X. Protective effects of quercetin on liver injury induced by ethanol. *Pharmacogn Mag*. 2010;6(22):135-141.
93. Li Z, Li Y, Zhang HX, *et al.* Mitochondria-Mediated Pathogenesis and Therapeutics for Non-Alcoholic Fatty Liver Disease. *Mol Nutr Food Res*. 2019;63(16):e1900043.
94. Peres W, Tuñón MJ, Collado PS, Herrmann S, Marroni N, González-Gallego J. The flavonoid quercetin ameliorates liver damage in rats with biliary obstruction. *J Hepatol*. 2000;33(5):742-750.
-

الملخص العربي

دور الكيرسيتين في تحسين السمية الكبدية المحدثه بسلفونات بيرفلور أكتان في ذكور الجرذان البيضاء البالغة (دراسة كيميائية حيوية و هستولوجية و هستوكيميائية مناعية)

داليا عبد الحميد مندور، مروة صبرى عبد العال، ابراهيم امين ابراهيم، رانيا سعيد معوض

قسم التشريخ و الاجنة، كلية الطب البشرى، جامعة الزقازيق

الخلفية: يعتبر بيرفلورو ألكيل وبولي فلورو ألكيل من المواد الكيميائية المصنعة المفورة و تشمل على بيرفلورو أكتان سلفونات و حمض بيرفلورو أوكتانويك. و تسبب هذه المواد سمية بيئية كامنة و يعتبر الكيرسيتين من الفلافونويد الاساسية الموجودة فى كثير من الطعام و لها خواص مضادة للأكسدة و مضادة للالتهابات.

الهدف من البحث: هدفت هذه الدراسة إلى توضيح الدور الوقائى المحتمل للكورسيتين ضد التغيرات النسيجية و الهستوكيميائية المناعية في الكبد التي يسببها سلفونات البيرفلور أكتان في ذكور الجرذان البيضاء البالغة.

المواد والطرق: تم توزيع ستة وثلاثين ذكوراً من الجرذان البيضاء بشكل متساوي و عشوائى إلى ثلاث مجموعات: المجموعة الضابطة. المجموعة المعالجة بسلفونات البيرفلور أكتان تمت اعطاؤها سلفونات البيرفلور أكتان عن طريق الفم) ٢٠ مجم / كجم / يوم (لمدة ٢٨ يوم. اما المجموعة الثالثة فقد تناولت كلا من الكورسيتين و سلفونات البيرفلور أكتان لمدة ٢٨ يوم. و في نهاية التجربة ، تم تخدير الجرذان و تم التضحية بها ، و مررت عينات الكبد لدراستها بالطرق الكيميائية الحيوية و الهستولوجية و الهستوكيميائية المناعية.

النتائج: في المجموعة المعالجة بسلفونات البيرفلور أكتان كان هناك انخفاض ذو دلالة احصائية فى وزن الجسم و فى مستوى انزيم أكسيد الديسموتاز الفائق (SOD) ، والجلوتاثيون بيروكسيداز (GPX) ، و الأنزيم المحفز (CAT) بينما كان هناك زيادة ذات دلالة احصائية فى وزن الكبد و زادت معدلات و وظائف الكبد و ايضا زاد مستوى مالونالدهيد (MDA) و ايضا البروتين التفاعلى (CRP) (C) و أظهر الفحص الميكروسكوبى تسلاً خلويًا التهابيًا و ظهرت فجوات فى الخلايا الكبدية و أنوية مشوهة الشكل و كان هناك العديد من الجسيمات المحللة و تضخم فى الميتوكوندريا تم أيضا الكشف عن تفاعل إيجابي قوي لكاسباس ٣ (Caspase ٣) و لعامل نخر الورم ألفا (TNF- α). و أظهرت المجموعة المعالجة بالكورسيتين بالإضافة الى سلفونات البيرفلور أكتان إعادة ضبط للقياسات الكيميائية الحيوية وتخفيف جزئى للنتائج الهستولوجية.

الخلاصة: يمكن أن يسلط هذا العمل الضوء على إمكانية استخدام الكورسيتين كاستراتيجية وقائية للسمية الكبدية المحتملة المحدثه بسلفونات البيرفلورو.